ELSEVIER

Biophysical Chemistry 115 (2005) 267–276

Biophysical Chemistry

http://www.elsevier.com/locate/biophyschem

Towards a new therapeutic target: *Helicobacter pylori* flavodoxin

Nunilo Cremades[a,b], Marta Bueno[a,b], Miguel Toja[c], Javier Sancho[a,b,*]

[a]*Biocomputation and Complex Systems Physics Institute, Spain*
[b]*Departamento de Bioquímica y Biología Molecular y Celular, Facultad de Ciencias, Universidad de Zaragoza, 50009-Zaragoza, Spain*
[c]*Operon S.A. Cuarte de Huerva, Zaragoza, Spain*

Received 28 June 2004; received in revised form 5 November 2004; accepted 10 December 2004
Available online 7 January 2005

Abstract

Helicobacter pylori flavodoxin is the electronic acceptor of the pyruvate–oxidoreductase complex (POR) that catalyzes pyruvate oxidative decarboxilation. Inactivation of this metabolic route precludes bacterial survival. Because flavodoxin is not present in the human host, substances interfering electronic transport from POR might be well suited for eradication therapies against the bacterium. *H. pylori* flavodoxin presents a peculiar cofactor (FMN) binding site, compared to other known flavodoxins, where a conserved aromatic residue is replaced by alanine. A cavity thus appears under the cofactor that can be filled with small organic molecules. We have cloned *H. pylori fldA* gene, expressed the protein in *Escherichia coli* and characterized the purified flavodoxin. Thermal up-shift assays of flavodoxin with different concentrations of benzylamine, as well as fluorescence titration experiments indicate benzylamine binds in the pocket near the FMN binding site. It seems thus that low affinity inhibitors of *H. pylori* flavodoxin can be easily found that, after improvement, may give rise to leads.

Keywords: Small molecule binding; *Helicobacter pylori*; Flavodoxin; Drug design; Protein stability; Protein cavity

1. Introduction

For most of the twentieth century, ulcers were thought to be caused by stress and dietetic factors but, in 1982, a link was established between a bacterium, *Helicobacter pylori*, and gastritis and stomach ulcers [1]. *H. pylori* is a Gram-negative bacterium specialized in the colonisation of the human stomach, a unique ecological niche characterized by a very acidic pH, where the bacterium establishes a life-long chronic infection [2]. *H. pylori* is one of the most common human pathogens and it has been detected in 50% of the world population [3]. Most infected people are, however, asymptomatic, and only 20% develop severe gastroduodenal pathologies, including type B gastritis, stomach and duodenal ulcers [4], adenocarcinomas [5] and stomach lymphomas [6]. Discovery of the genetic variability of *H. pylori* [7] sheds light on this unexpected finding and suggests that if antibiotics are used extensively, the target bacterium is likely to develop resistance [8]. The current treatment consists of a triple [9], sometimes quadruple therapy, combining a proton inhibitor and two (or three) antibiotics. New cases of resistance are continuously reported [10–13] and, therefore, new treatments need to be developed [14–16]. Efforts to find a human vaccine against *H. pylori* [17–19] encounter difficulties characteristic of the reported genetic variability. Looking for new molecular targets to develop new drugs against the pathogen [20] is, thus, an obvious goal.

Towards that end, we notice that the *H. pylori* genome contains a small redox protein, flavodoxin, which is encoded by the *fldA* gene [21]. *H. pylori* flavodoxin functions as an electron acceptor of the pyruvate–oxidoreductase (POR) enzyme complex, which catalyses the oxidative decarboxilation of pyruvate [22]. Pyruvate is an

* Corresponding author. Departamento de Bioquímica y Biología Molecular y Celular, Facultad de Ciencias, Universidad de Zaragoza, Pedro cerbuna 12, 50009-Zaragoza, Spain. Tel.: +34 976761286; fax: +34 976762123.
E-mail address: jsancho@unizar.es (J. Sancho).

0301-4622/$ - see front matter © 2004 Elsevier B.V. All rights reserved.
doi:10.1016/j.bpc.2004.12.045

important intermediate in the physiology of the bacterium as it constitutes a branch point of several metabolic routes [23]. Recent work has reported the crystal structure of *H. pylori* flavodoxin and has demonstrated that both, flavodoxin and the POR complex, are essential for bacterium survival [24]. A second requirement for the new molecular target should be its absence in the human host. Flavodoxins have been identified in both prokaryotes [25] and eukaryotes [26] but not in mammals, where flavodoxin-like domains are found as part of larger proteins such as *P*450 reductase [27]. Besides, the flavodoxin has been proposed to play a potential role in the pathogenesis of MALT lymphoma, being detected in the sera of a high percentage of patients with MALToma compared to patients with other diseases related with *H. pylori* [28]. Flavodoxin thus seems a promising candidate to be a target to develop drugs suited for the eradication of the bacterium.

Our laboratory has used over the years the flavodoxin from a different specie (*Anabaena* PCC7119) as a model protein to investigate protein stability, protein folding and binding [29–35]. From the structural point of view, flavodoxins are α/β proteins and bind at the C-terminal end of the β-sheet, a molecule of flavin mononucleotide (FMN) that confers redox properties to the protein [36]. The redox potentials of FMN are drastically altered by the protein environment, making possible the one-electron reduction of the cofactor, which is essential for protein function. The different flavodoxins are usually classified in two groups: short-chain flavodoxin (with around 150 residues) and long-chain flavodoxin (with an insertion of 20 residues in the fifth strand of the β-sheet [37]). *H. pylori* flavodoxin belongs to the long-chain group, like that from *Anabaena*. The two proteins share a 43% sequence identity (Fig. 1a). Although the overall fold of *H. pylori* flavodoxin is similar to that of other known flavodoxin, its FMN binding site is peculiar (Fig. 1b) because it contains, in one of the cofactor binding loops, an alanine residue where a vast majority of flavodoxins display an aromatic residue, typically a tryptophan. This makes the FMN of *H. pylori* flavodoxin partly accessible to solvent through a pocket at the protein surface where small molecules could bind and inhibit protein function, and thus, bacterium growth. The inhibitory effect could be exerted either by modifying the environment of the FMN and thus, altering the redox potentials [38] or simply, if the ligand is bulky enough, by interfering with flavodoxin

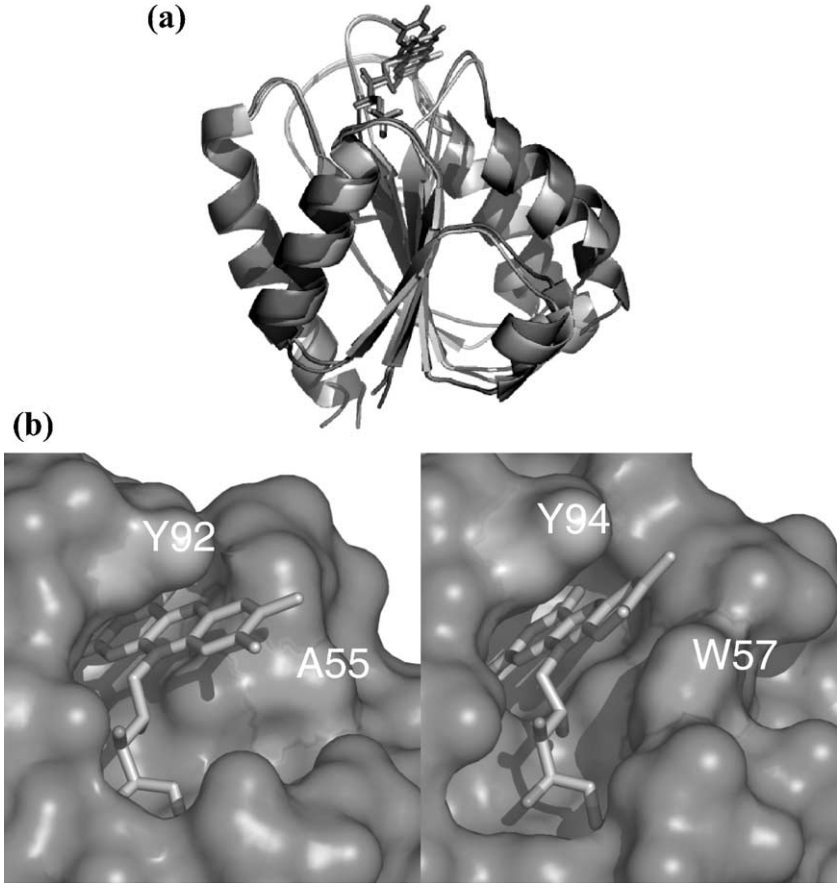

Fig. 1. (a) *Helicobacter pylori* flavodoxin structure (1FUE, in light grey) superimposed on the *Anabaena* PCC7119 flavodoxin structure (1FLV, dark grey). (b) Surface accessibility of the cofactor binding site in: (right) *H. pylori*, (left) *Anabaena* sp. The absence of the indole group of the tryptophan residue creates a cavity in the protein that is only partially closed by the cofactor. FMN is represented in sticks. Positions in contact with the cofactor are highlighted.

recognition by the POR partner complex. We begin here exploring this possibility by testing the binding of small molecules to the pocket near the FMN binding site in *H. pylori* flavodoxin.

2. Experimental

2.1. DNA isolation, and PCR amplification of the fldA gene

Total genomic DNA was isolated from three different *H. pylori* antigen-positive stool samples and three negative matched controls using *QIAamp* DNA *Stool Mini Kit* (*Qiagen*). *H. pylori* antigen status was ascertained by ELISA, using *Premier Platinum Stool Antigen* detection test *HpSA*, and by immunochromatography using *Immunocard STAT HpSA* (*Meridian Diagnostics*). Then, the *H. pylori* flavodoxin DNA coding sequence was amplified by PCR, using the Nco-5′ Primer: GGATTGAGCATATGGGAAAAATTGG and the *Bam*HI 3′ primer: CTAACAATGAAGGATCCAATTCTAG. Both primers were derived from the directly submitted J99 *fldA* sequence (accession number AF221524 [39]) obtained from the Genebank (EMBL) database. The reaction mixture (50 μl) contained undigested chromosomal DNA, 1 μg; primers, 50 ng; dNTP mixture, 2 mM; 10-fold-concentrated amplification buffer, 5 μl and *Taq* DNA polymerase (*Madgen*), 1.5 units. Thirty-five cycles of 2-min hybridization at 44 °C, 1-min extension at 72 °C and 1-min denaturation at 94 °C were performed. After amplification, fragments of approximately 600 nucleotides were identified in two *H. pylori* positive amplifications, corresponding to the predicted 613 nucleotides fragment. The fragments were gel-purified and cloned into the *Nco*I–*Bam*HI sites of the pET28a expression vector (*Novagen*) using standard techniques. Several clones were obtained in *E. coli* JM109, sequenced and used for protein expression.

2.2. Recombinant overexpression and purification of H. pylori flavodoxin

E. coli expression strain BL21 containing the pET28a-*fldA* plasmid was grown in 10 ml of Luria-Bertani medium in the presence of 0.2 mg kanamycine. The culture was diluted 10-fold in the same conditions and cells were grown to an absorbance of 0.8 at 600 nm. At this point, isopropyl β-D-thiogalactoside (IPTG) was added to a final concentration of 1 mM and the cells were allowed to grow for at least 3 h and then pelleted and washed once with 0.15 M NaCl. After centrifugation, the cells were dissolved in 50 mM Tris–HCl buffer, pH 8, containing 1 mM β-mercaptoethanol, 1 mM EDTA and 1 mM PMSF (phenylmethanesulphonyl fluoride). The cells were disrupted by ultrasonic treatment (four periods of 45 s, with 30-s intervals). Debris and unbroken cells were removed by centrifugation (45 min at 18000 rpm at 4 °C). Then, the supernatant was precipitated with 65% $(NH_4)_2SO_4$ as first step of purification.

After precipitation with 65% saturated $(NH_4)_2SO_4$, the remaining supernatant was poured onto a DE-52 DEAE-cellulose column equilibrated with 65% saturated $(NH_4)_2SO_4$ in 50 mM Tris–HCl buffer, pH 8. *H. pylori* flavodoxin binds to the column as a yellow band. The protein was eluted with a reverse gradient of the equilibration buffer from 65% to 0% $(NH_4)_2SO_4$ saturation. After dialysis, flavodoxin fractions were poured onto a DE-52 DEAE-cellulose column previously equilibrated with 50 mM Tris–HCl buffer, pH 8. A nearly pure flavodoxin was eluted with a linear gradient of 0 to 0.5 M NaCl in 50 mM Tris–HCl buffer, pH 8. Finally the protein was concentrated in a MonoQ10 column (*FPLC*, *Amersham*) equilibrated with 50 mM Tris–HCl buffer, pH 8, and then eluted with a linear gradient of 0 to 1 M NaCl. The protein was pure according to SDS-PAGE and to the ratio of UV to visible absorbance.

In addition, the *Anabaena* flavodoxin W57A mutant, where the highly conserved tryptophan residue of the FMN binding site is substituted by alanine, was expressed and purified as described [30].

2.3. Determination of extinction coefficients

The extinction coefficient of *H. pylori* flavodoxin in the fully oxidized state was determined as described by Mayhew and Massey [40] using, for released FMN, a corrected extinction coefficient at 445 nm of 12020 M^{-1} cm^{-1}, in 10 mM phosphate buffer pH 7 and of 12070 M^{-1} cm^{-1}, in 50 mM Tris–HCl pH 8. All extinction coefficients, as well as the correction factor, were determined in triplicate. Determination of its extinction coefficient shows quite similar values at different conditions. The extinction coefficient (at 25±0.1 °C) at 452 nm is of 10650 M^{-1} cm^{-1} in 50 mM Tris–HCl buffer pH 8 and of 10490 M^{-1} cm^{-1} in 10 mM phosphate buffer pH 7.

2.4. Spectroscopic characterization

UV/Visible absorbance; UV/Visible fluorescence emission; far-UV, near-UV and visible circular dichroism (CD) measurements were carried out at 25±0.1 °C and pH 7.0 in 10 mM phosphate buffer. The UV/Vis spectra were recorded in a *Uvikon* 942 UV–Visible spectrophotometer from *Kontron Instruments*. Fluorescence emission spectra (300 to 400 nm) were recorded, with excitation at 280 nm, using an *Aminco-Bowman Series* 2 spectrometer. Fluorescence emission spectra, in the visible region (from 500 to 600 nm), were also recorded with excitation at 453 nm. CD spectra in the near-, far-UV and visible were recorded in a *Jasco 710* spectropolarimeter. All experiments were carried out in darkness.

2.5. Thermal up-shift assay

Thermal denaturation was followed by recording FMN fluorescence emission (525 nm, with excitation at 453 nm) in an *Aminco-Bowman Series 2* spectrometer. Protein concentration was 10 μM in 10 mM phosphate buffer, pH 7.

Thermal denaturation curves were fitted to a two-state equation:

$$S = \frac{S_N + m_N T + (S_U + m_U T)\exp^{-\Delta G(T)/RT}}{1 + \exp^{-\Delta G(T)/RT}} \quad (1)$$

where S_N and S_U represent the spectroscopic signals of the native and unfolded states at 0 K, and m_N and m_U are the temperature dependences of those signals. The Gibbs energy function, $\Delta G(T)$, is given as:

$$\Delta G(T) = \Delta H_{T_m}(1 - T/T_m) - \Delta C_p((T_m - T) + T\ln(T/T_m)) \quad (2)$$

with ΔC_p and ΔH_{T_m} being the unfolding heat capacity and enthalpy changes at T_m, respectively. Fitting thermal unfolded curves to Eq. (1) provides accurate values of T_m, reasonable ΔH_{T_m} values and usually unreliable ΔC_p values. It should be noticed that, although the visible fluorescence thermal unfolding of the protein can be fitted to two-state model, the global thermal unfolding of *H. pylori* flavodoxin is not two-state (unpublished). Therefore, the reported T_m values are apparent.

In order to carry out the thermal up-shift assay, flavodoxin denaturations were performed in the absence and in presence of different concentrations of ligand (after 14 h of equilibration). The ligand binding affinity was estimated from the change induced by the ligand in the unfolding transition temperature. First, fluorescence emission unfolding curves recorded in both absence and presence of ligand were fitted to Eq. (1) and the corresponding thermodynamic parameters obtained. Then, the ligand binding constant at the apparent melting temperature (K_{T_m}) was calculated using the expression described by Brandts and Lin [41]:

$$K_{T_m} = \frac{\exp\left[\frac{-\Delta H_u}{R}\left(\frac{1}{T_m} - \frac{1}{T_0}\right) + \frac{\Delta Cp_u}{R}\left(\ln\frac{T_m}{T_0} + \frac{T_0}{T_m} - 1\right)\right]}{[L_{T_m}]} \quad (3)$$

where ΔH_u and ΔCp_u are, respectively, the unfolding enthalpy and heat capacity changes at the melting temperature in the absence of ligand, T_0 and T_m the melting temperatures in the absence and presence of ligand, R the ideal gas constant and $[L_{T_m}]$ the concentration of free ligand at T_m ($[L_{T_m}] \cong [L]_{tot}$ when $[L]_{tot} \gg [Protein]_{tot}$). To compare the binding affinities obtained from thermal up-shift assays with those derived from the ligand titrations, the K_{T_m} values have to be extrapolated to the titration temperature. For that, we use the expression suggested by Pantoliano et al. [42]:

$$K_T = K_{T_m}\exp\left[\frac{-\Delta H}{R}\left(\frac{1}{T} - \frac{1}{T_m}\right)\right] \quad (4)$$

where ΔH_L^T is the binding enthalpy at the temperature T.

2.6. Dissociation constants

Dissociation constants of the flavodoxin–ligand complexes were directly determined by titration, followed fluorometrically (excitation was at 464 nm, and the emission was recorded at 525 nm) in an *Aminco-Bowman Series 2* spectrometer at 25±0.1 °C (in darkness). Protein samples were prepared by mixing 900 μl ligand solution of different concentrations with 100 μl aliquots of 40 μM holoprotein, in 10 mM sodium phosphate, pH 7.0 and were allowed to equilibrate for 14 h. Ligand binding, presumably at the pocket of the FMN binding site, quenches the cofactor fluorescence emission. The dissociation constants were calculated using Origin 6.0 (*OriginLab*) by fitting the emission fluorescence data to equation:

$$F = F_p + \frac{(F_c - F_p)}{2C_p} \times \left(C_p + C_L + K_d - \sqrt{(C_p + C_L + K_d)^2 - 4C_pC_L}\right) + BC_L \quad (5)$$

where F is the observed fluorescence emission intensity of each solution, F_p the emission of the protein, F_c the emission of the complex, C_p the total protein concentration, K_d the dissociation constant of the complex in micromolar units, C_L the total concentration of ligand in each solution, and B a constant (to fit the experimental final slope at high ligand concentrations). The robustness of the fits is indicated by the fact that the total concentration of protein, when treated as unknown, was correctly predicted (within 90%).

3. Results and discussion

3.1. Cloning, overexpression and purification

The *H. pylori fldA* gene was amplified using PCR. To design the oligonucleotides, the information available in the Genebank (EMBL) for *H. pylori* J99 strain was used. Two oligonucleotides, complementary to the beginning and to the end of the *fldA* gene, bearing *Nco*I and *Bam*HI restriction sites were synthesized. After amplification, a single band of approximately 600 nucleotides (Fig. 2) was identified.

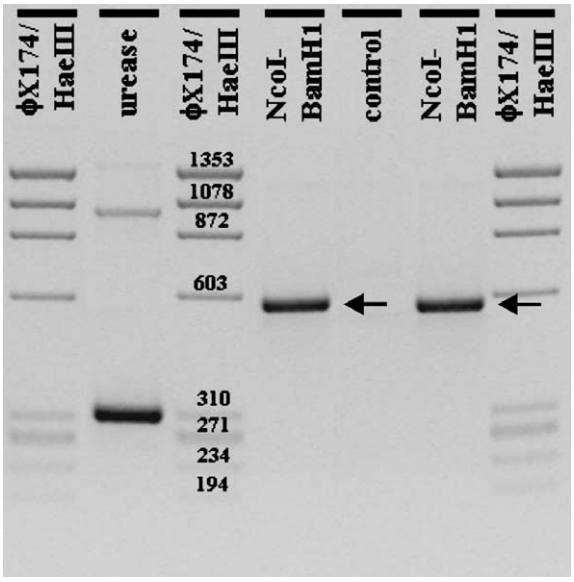

Fig. 2. Ethidium bromide-stained agarose gel displaying the results of PCR amplification of *fldA* gene. In order to check the conditions of *H. pylori* genomic DNA sample, amplification of a control gene codifying urease was carried out. Amplification without DNA was used as a negative control. The molecular weight marker used was ϕX174/HaeIII (*Stratagene*). Arrows mark the product amplified.

The protein was purified to homogeneity from a bacterial extract using three anion exchange chromatography steps. Denaturant gel electrophoresis analysis revealed one major band with a molecular weight of 18 kDa (data not shown), which is in agreement with the expected value of 17.9 kDa.

3.2. Spectroscopic properties of H. pylori holoflavodoxin

H. pylori holoflavodoxin displays a characteristic absorbance spectrum in the visible (Fig. 3a) due to the bound FMN cofactor, with maxima at 378 nm and 452 nm. The near UV maximum is at 271 nm. The main near-ultraviolet and visible absorbance properties of *H. pylori* flavodoxin are compared to those of WT and W57A *Anabaena* flavodoxin in Table 1. We noticed that mutation of the *Anabaena* W57 residue to alanine does not make the spectrum of *Anabaena* flavodoxin closer to that of the *H. pylori* protein. This suggests that the higher resemblance of the visible spectrum of *H. pylori* flavodoxin to that of FMN (compared to that of *Anabaena* flavodoxin) in not related to the lack of a tryptophan residue at the FMN binding site. A comparison of the *H. pylori* (1FUE) and WT *Anabaena* flavodoxin (1FLV) X-ray structures does not offer clues for the differences in visible spectrum of the two flavodoxins, because both the tyrosine/FMN stacking and the hydrogen bonding pattern are similar. However, solvent-accessible surface calculation indicates that the FMN in the *H. pylori* flavodoxin is far more accessible to water molecules, that in other long-chain flavodoxins (160 $Å^2$ for *H. pylori* flavodoxin and between 99 and 109 $Å^2$ for the others [24]). This fact could explain the observed resemblance between the *H. pylori* flavodoxin and FMN spectra.

H. pylori flavodoxin contains two tryptophan residues. Upon excitation of the protein at 280 nm, the maximum fluorescence emission in native conditions (25 °C) appears at 322 nm (Fig. 3b). This indicates that tryptophans are shielded from the solvent in the folded conformation, as can be observed in the X-ray structure. Heating the protein to 90 °C leads to a shift of the fluorescence emission maximum to 344 nm, indicative of partial unfolding. The fluorescence spectrum in the visible region is shown in Fig. 3c. Upon unfolding, the FMN is released and the quantum yield increases moderately. This moderate increase agrees with the fact that, unlike in other flavodoxins where the FMN is largely shielded from solvent (as is the case of the *Anabaena* protein), in *H. pylori* flavodoxin the bound cofactor is more solvent exposed and thus less quenched by protein residues.

The far-UV CD spectrum of flavodoxin in 10 mM phosphate pH 7.0 is shown in Fig. 3d. The ellipticity minimum at 222 nm is consistent with a substantial amount of secondary structure, which is largely, but not completely, lost upon heating to 90 °C. The spectrum is similar to that of the *Anabaena* flavodoxin where, in addition to secondary structure contributions, there are also contributions from aromatic residues. It should be noticed, in this respect, that the two proteins contain highly conserved clusters of aromatic residues.

The near-UV CD spectrum (Fig. 3e) shows distinct peaks, as is characteristic of a well-defined tertiary structure. The peaks are lost upon heating. This spectrum differs from that of *Anabaena* holoflavodoxin (unpublished) by having a very pronounced negative peak centred at 268 nm.

The visible CD spectrum (Fig. 3f) was recorded to further characterize the binding of the flavin mononucleotide (FMN) to the protein at 25 °C. The protein-induced asymmetric environment of FMN is lost upon heating.

3.3. Thermal stability of holoflavodoxin

Thermal unfolding of *H. pylori* and of WT and W57A *Anabaena* flavodoxins have been carried out to compare the thermal stability of the proteins. The fluorescence emission of the FMN in the visible region increases as a consequence of the unfolding. The fluorescence curves (Fig. 4) have been fitted to two-state models and apparent T_m have been calculated.

The melting temperatures obtained from the thermal profiles were 317 K for *H. pylori*, 328 K for the *Anabaena* W57A mutant and 340 K for *Anabaena* WT flavodoxin. The stability rises in this series mimic the increase in the affinity of the three apoflavodoxin-FMN

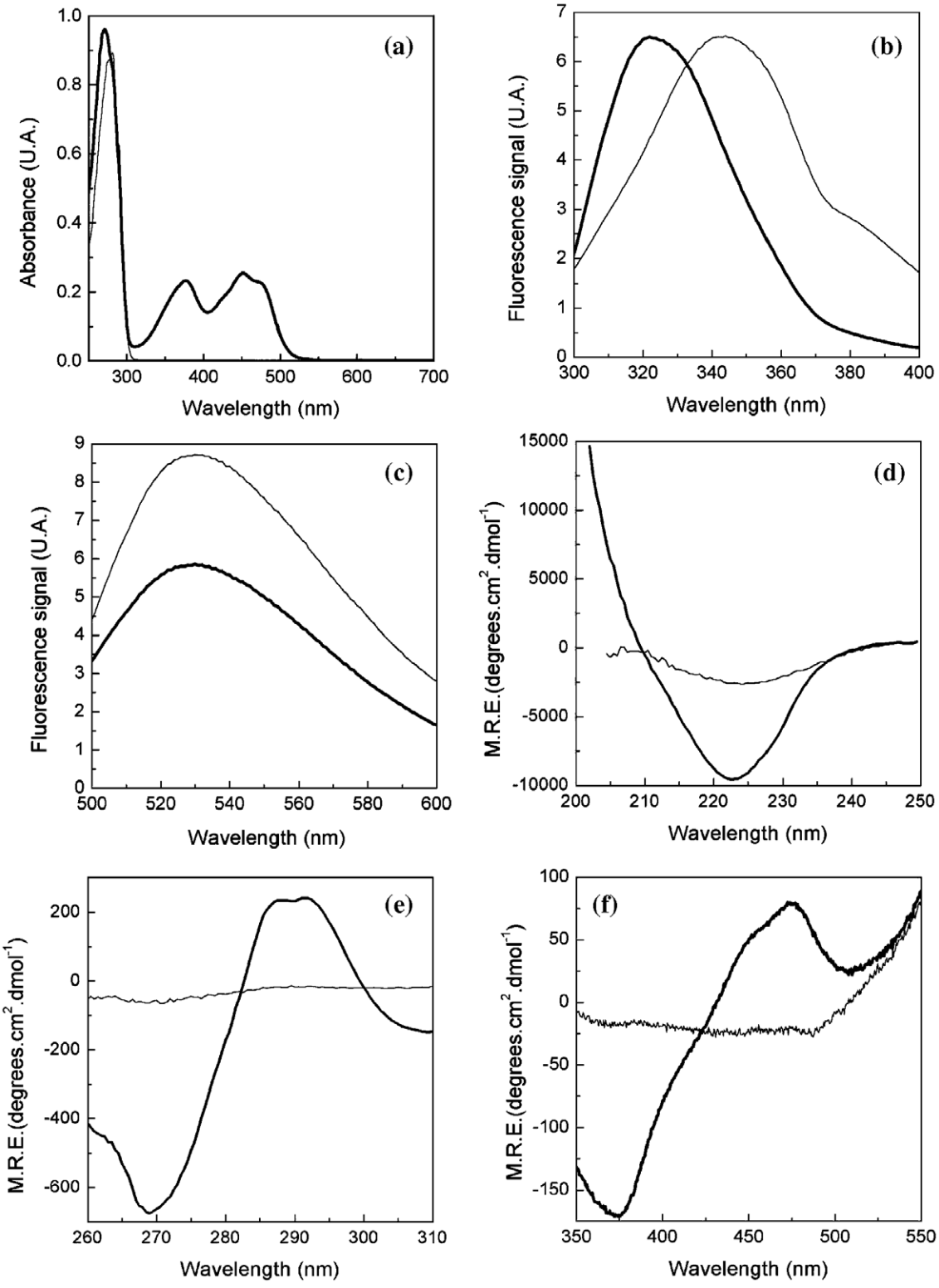

Fig. 3. *H. pylori* holoflavodoxin spectroscopic characterization. (a) UV/VIS absorbance of holo and apoflavodoxin (thick line). Spectral properties of the folded (thick line) and unfolded (90 °C, thin line) protein measured with different techniques. (b) UV fluorescence emission. (c) Fluorescence emission in the visible region. (d) Far-UV circular dichroism. (e) Near-UV circular dichroism. (f) Circular dichroism in the visible region.

complexes, which for the *Anabaena* WT is around 3 kcal mol^{-1} higher than for the W57A mutant and 4 kcal mol^{-1} higher than for the *H. pylori* one (data not shown). This increase in complex stability is expected, because any ligand that specifically binds the native state of a protein should stabilize it [43].

Table 1
UV/VIS spectral properties of the different flavodoxins characterized

Molecule	λ_{max} (nm)		λ_{min} (nm)	
	I	II	I	II
FMN	445	372	400	303
H. pylori flavodoxin	452	378	406	310
Anabaena WT flavodoxin	463	374	406	315
Anabaena W57A flavodoxin	460	373	407	315

3.4. Small molecule binding

The *H. pylori* flavodoxin crystal structure [24] is compared with the structure of the flavodoxin from the cyanobacteria *Anabaena* PCC7119 in Fig. 1a. Although the overall fold is conserved, there is an interesting difference at the FMN binding site. Usually, as in *Anabaena* flavodoxin, the isoalloxacine ring of FMN is embedded into the protein, stacked between two hydrophobic residues. All structurally known flavodoxins display a tyrosine residue at the re- and a tryptophan one at the si-face of the FMN molecule (except the *Clostridium beijerenckii* flavodoxin, with a methionine at the si- and a tryptophan at the re-face). This aromatic environment is a well-conserved feature of the FMN binding site that is altered in *H. pylori* flavodoxin, where the si-face is occupied by an alanine. As a consequence, the isoalloxacine ring is slightly rotated, compared to other flavodoxins, although, this does not affect the hydrogen-bonding pattern of the cofactor. The absence of the indole group of the tryptophan, replaced by alanine, at the si-face of the FMN in *H. pylori* flavodoxin creates a pocket in the vicinity of the cofactor. This makes the FMN group more accessible to solvent and yet, water molecules have not been found in the pocket in the crystal structure. Hence, small molecules could, in principle, bind in this pocket and inhibit protein function (either causing redox potential changes or, if bulky enough, through sterical constrains suppressing interactions with its partner protein) leading to inhibition of bacterial growth.

Work currently in progress in our laboratory has focused on the binding of small molecules to cavity-containing mutants of *Anabaena* flavodoxin. Our unpublished results indicated that, when the FMN is removed, its binding site can bind small ligands. For the *H. pylori* flavodoxin, we suspected that we could probably detect binding to the functional holoform by taking advantage of the pocket at the FMN site. We thus tested some small ligands and present here the results of benzylamine binding, a compound that combines the aromatic features of the missing binding site

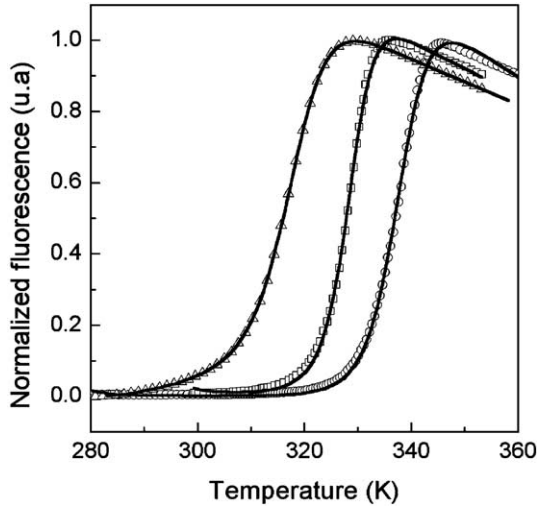

Fig. 4. Thermal denaturation curves of flavodoxin as followed by fluorescence emission of FMN: *Anabaena* wild type (circles), *Anabaena* W57A (squares), *H. pylori* (triangles). Solid lines represent the fitting of the data to a two-state model.

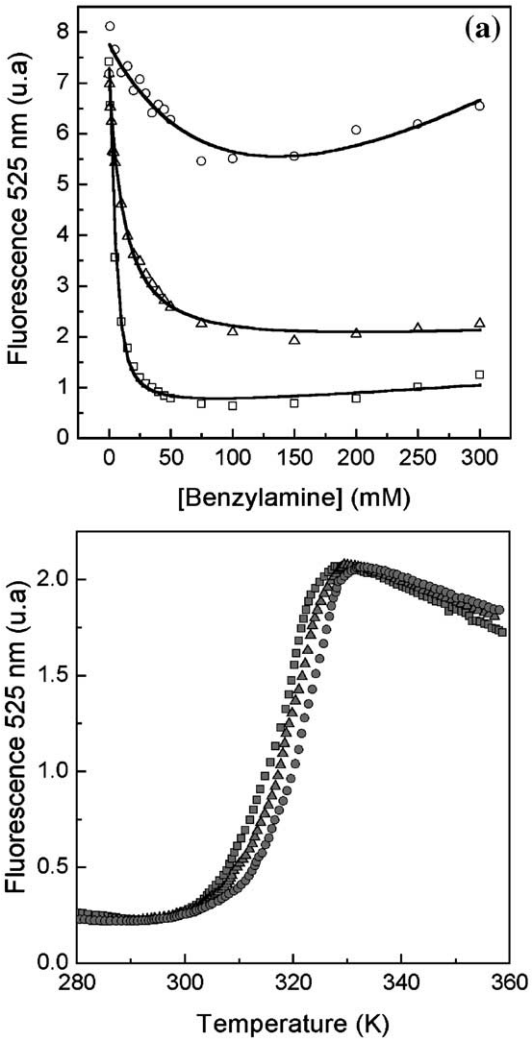

Fig. 5. (a) Titration of FMN fluorescence with benzylamine in *Anabaena* WT (circles), *Anabaena* W57A (squares) and *H. pylori* flavodoxin (triangles). Solid lines represent the fitting of the data to Eq. (3). (b) Thermal up-shift assays performed with *H. pylori* flavodoxin in presence of increasing amounts of benzylamine: absence of ligand (squares); 10 mM (triangles); and 50 mM (circles). The thermal curves were obtained following FMN fluorescence and then fitted to a two-state model.

Table 2
Thermal up-shift assays data

[L][a]	*Anabaena* WT		*Anabaena* W57A		*Helicobacter pylori*	
	T_m (K)[b]	ΔT_m (K)	T_m (K)	ΔT_m (K)	T_m (K)	ΔT_m (K)
0	340.1±0.1		328.5±0.0		317.4±0.2	
10	338.7±0.2	−1.4±0.2	329.6±0.1	1.1±0.1	319.8±0.1	2.3±0.2
50	339.3±0.1	−0.9±0.1	330.1±0.0	1.7±0.1	322.2±0.1	4.8±0.2

[a] Benzylamine concentration in mM.
[b] Calculated from fittings of flavodoxin thermal denaturation curves to a two-state model (Eqs. (1) and (2)).

tryptophan with the possibility of establishing cation/π interactions with the FMN [44].

First we tested binding of benzylamine to the W57A *Anabaena* mutant flavodoxin and observed marked quenching of FMN fluorescence in the presence of the ligand. The concentration dependence of the quenching (Fig. 5a) is consistent with complex formation. The binding seems to occur close to the FMN, as indicated by the quenching. Calculation of the dissociation constant by ligand titration gave a value around 4 kcal mol^{-1} for the benzylamine *Anabaena* W57A complex. When the binding of benzylamine to *H. pylori* flavodoxin was tested, we also found a marked quenching and the calculated binding of energy was around 3 kcal mol^{-1} (Table 3).

To confirm benzylamine binding, we performed thermal up-shift assays. These assays measure ligand binding-dependent protein stabilization, as monitored by T_m measurements of the melting transitions of ligand–protein complexes, and of the uncomplexed protein. Protein stabilization by ligand binding is related to ligand binding affinity (ΔG_{bind}) because of the thermodynamic linkage between the binding and unfolding equilibria [45,46].

As shown in Table 2, thermal up-shift assays can detect ligand binding. Small and negative T_m shifts are detected for the wild type *Anabaena* holoflavodoxin that should be attributed either to binding to non-native conformations or to effects exerted through modifying water structure. In contrast the thermal melting transition of *H. pylori* flavodoxin was increased by 5 K in the presence of 50 mM benzylamine, while in the *Anabaena* W57A mutant, the shift was only of 2 K.

The calculation of binding constants, from thermal denaturation data, is based on two assumptions: all transitions are two-state in character, and ligands bind only to the nature state with a 1:1 stoichiometry [41]. All the parameters needed to calculate dissociation constants at 298 K are taken from the fits of the unfolding curves. The ligand binding enthalpy is the only parameter not experimentally determined from thermal melting transitions. For a majority of ligand/protein binding enthalpy measurements reported in the literature, however, an average near to −10 kcal mol^{-1} to −15 kcal mol^{-1} has been observed [47,48]. In the absence of any other information, we assume that −15 kcal mol^{-1} can be used to make reasonable estimates of K_T [42].

No binding constant can be calculated for *Anabaena* WT because of the negative shift observed in the melting transition temperature. Binding energies obtained by thermal shift assays agree well with those obtained by direct equilibrium methods (as titration) when they are extrapolated to identical temperature (−3.8 kcal mol^{-1} and −3.9 kcal mol^{-1}, respectively) for *Anabaena* W57A (Table 3). Nonetheless, for *H. pylori* there is some difference between the energies calculated by titration (−2.7 kcal mol^{-1}) and by thermal denaturation (−4.2 kcal mol^{-1}), possibly due to the uncertainty in the estimated enthalpy of ligand binding.

3.5. *H. pylori flavodoxin as a new drug target*

The genetic diversity of the *H. pylori* species is large. Simultaneous infection with multiple strains of *H. pylori* that can exchange genetic sequences is common [49]. The development of clinically manifest disease during chronic infection seems to result from complex and poorly understood interactions among a number of factors, including the susceptibility of the host and the virulence of the infecting strains [50].

Triple therapy has been the most successful method for eradicating *H. pylori* (eradication rate of 80–90%). However, increasing metronidazole resistance has limited the

Table 3
Dissociation constants at 25 °C calculated by titration and thermal up-shift assays

Protein	Titration		Thermal up-shift assay	
	K_d[a] (mM)	ΔG (kcal/mol)	K_d[b] (mM)	ΔG (kcal/mol)
Anabaena WT	143.7±85.3	−1.1±0.4	Nd[c]	Nd
Anabaena W57A	1.7±0.3	−3.8±0.1	1.2±0.5	−3.9±0.2
H. pylori	9.8±1.3	−2.7±0.1	0.9±0.3	−4.2±0.2

[a] Directly determined by fluorescence titration (excitation at 464 nm, and emission at 525 nm) using Eq. (5).
[b] Indirectly obtained from thermal up-shift assays (Eq. (3)), extrapolating from binding constants calculated at the melting temperature (Eq. (4)).
[c] Not determined.

expansion of this therapy [51]. The activation of metronidazole, inside the bacteria, is closely linked to the oxidation of pyruvate [52] and requires reduction of the nitro group of nitroimidazole to generate the entity that kills susceptible bacteria. In aerobic conditions, this reduction is mediated by the POR complex. Electrons liberated in the oxidation of pyruvate are first transferred to flavodoxin, from where they can be delivered to metronidazole. The short-lived reaction products formed can react with DNA, causing strand breaking and subsequent cell death [53].

The problem associated to metronidazole resistance could be avoided by focusing on new targets. One obvious possibility is to block *H. pylori* electron transfer reactions at the flavodoxin level. Ligand binding near the FMN flavodoxin cofactor could easily disrupt electron transfer either by altering the redox potentials or by impeding the recognition of the POR-complex (which most likely will take place near the FMN site). Since the surface exposed region of the cofactor binding site is small and highly conserved among the flavodoxins of different species and, additionally, it constitutes the binding site of partner flavodoxin proteins, we hope inhibitors designed to bind there should resist genetic variability. Our preliminary study indicates that it is not difficult to identify small molecules, such as benzylamine, which bind to the *H. pylori* pocket, and thus may constitute leads towards inhibiting flavodoxin function. As the affinity of these molecules may be low, known methods of redesigning ligands for higher affinity will be needed [45].

Acknowledgements

Spanish Ministry of Education Fellowhips supported NC and MB. We thank L.A. Campos and A. Velázquez for stimulating discussion. We acknowledge financial support from grants BCM2001-252 (DGI, Spain) and P120/2001 (DGA, Spain).

References

[1] J.R. Warren, B.J. Marshall, Unidentified curved bacilli on gastric epithelium in active chronic gastritis, Lancet 1 (1983) 1273–1275.
[2] R.A. Feldman, in: M. Achtman, S. Suerbaum (Eds.), *Helicobacter Pylori*: Molecular and Cellular Biology. Epidemiologic Observations and Open Questions About Disease and Infection Caused by *Helicobacter Pylori*, Horizon Scientific, Norfolk, 2001.
[3] J. Parsonnet, The incidence of *Helicobacter pylori* infection, Aliment. Pharmacol. Ther. 9 (suppl. 2) (1995) 45–51.
[4] M.J. Blaser, Hypotheses on the patogenesis and natural history of *Helicobacter pylori*-induced inflammation, Gastroenerology 102 (1992) 720–727.
[5] J. Parsonnet, G.D. Friedman, D.P. Vandersteen, Y. Chang, J.H. Vogelman, N. Orentreich, R.K. Sibley, *Helicobacter pylori* infection and the risk of gastric carcinoma, N. Engl. J. Med. 325 (1999) 1127–1131.
[6] A.C. Wotherspoon, C. Doglioni, T.C. Diss, L. Pan, A. Moschini, M. de Boni, P.G. Isaacson, Regression of primary low-grade B-cell gastric lymphoma of mucosa-associated lymphoid tissue type after eradication of *Helicobacter pylori*, Lancet 342 (1993) 575–577.
[7] D.E. Taylor, M. Eaton, N. Chang, S.M. Salama, Construction of a *Helicobacter pylori* genome map and demonstration of diversity at the genome level, J. Bacteriol. 174 (1992) 6800–6806.
[8] Y. Glupczynski, A. Burette, Drug therapy for *Helicobacter pylori* infection: problems and pitfalls, Am. J. Gastroenterol. 85 (1990) 1545–1551.
[9] K. Seppala, H. Nuutinen, New options in eradication of *Helicobacter pylori*, Ann. Med. 27 (1995) 601–604.
[10] S. Mendonca, C.C. Ecclissato, M.S. Sartori, A.P. Godoy, R.A. Guersoni, M. Deguer, J. Pedrazzoli, Prevalence of *Helicobacter pylori* resistance to metronidazole, clarithromycin, amoxycillin, tetracycline, and furazolidone in Brazil, Gastroenterology 118 Part 2 (Suppl. 2) (2000) 5822.
[11] J.J. Kim, R. Reddy, S.G. Reddy, F.A. El-Zaatari, M.S. Osato, J.G. Kim, D.Y. Graham, D.H. Kwon, Increasing *Helicobacter pylori* resistance to metronidazole, clarithromycin and tetracycline, Gastroenterology 118 Part 1 (Suppl. 2) (2000) 2671.
[12] R.J. Adamek, S. Suerbaum, B. Pfaffenbach, W. Opferkuch, Primary and acquired *Helicobacter pylori* resistance to clarithromycin, metronidazole, and amoxicillin—influence on treatment outcome, Am. J. Gastroenterol. 93 (1998) 386–389.
[13] F. Megraud, *Helicobacter pylori* resistance to antibiotics, Presse Med. 26 (1997) 1775–1780.
[14] F. Megraud, Resistance of *Helicobacter pylori* to antibiotics: the main limitation of current proton-pump inhibitor triple therapy, Eur. J. Gastroen. Hepatol. 11 (Suppl. 2) (1999) S35–S37.
[15] F. Megraud, J. Laurent, J.F. Flejou, A. Caekaert, P. Barthelemy, *Helicobacter pylori* resistance to antimicrobial agents after treatment failure with omeprazole triple therapy, Gastroenterology 116 (Part 2) (1999) G0519.
[16] K. Murakami, T. Fujioka, T. Kubota, R. Sato, M. Kodama, M. Kimoto, M. Nasu, Prevalence of acquired *Helicobacter pylori* resistance to clarithromycin and combinations of eradication regimens, Gastroenterology 116 (Part 2) (1999) G1138.
[17] M.F.T. Rupnow, R.D. Shachter, D.K. Owens, J. Parsonnet, Quantifying the population impact of a prophylactic *Helicobacter pylori* vaccine, Vaccine 20 (2001) 879–885.
[18] J.S. Kim, J.H. Chang, S.I. Chung, J.S. Yum, Importance of the host genetic background on immune responses to *Helicobacter pylori* infection and therapeutic vaccine efficacy, FEMS Immunol. Med. Microbiol. 31 (2001) 41–46.
[19] C. Hatzifoti, *Helicobacter pylori* vaccine strategies—triggering a gut reaction, Trends Immunol. 22 (2001) 225.
[20] P. Legrain, D. Strosberg, Protein interaction domain mapping for the selection of validated targets and lead compounds in the anti-infectious area, Curr. Pharm. Des. 8 (2002) 1189–1198.
[21] R.A. Alm, L.S. Ling, D.T. Moir, B.L. King, E.D. Brown, P.C. Doig, D.R. Smith, B. Noonan, B.C. Guild, B.L. deJonge, G. Carmel, P.J. Tummino, A. Caruso, M. Uria-Nickelsen, D.M. Mills, C. Ives, R. Gibson, D. Merberg, S.D. Mills, Q. Jiang, D.E. Taylor, G.F. Vovis, T.J. Trust, Genomic-sequence comparison of two unrelated isolates of the human gastric pathogen *Helicobacter pylori*, Nature 397 (1999) 176–180.
[22] N.J. Hughes, C.L. Clayton, P.A. Chalk, D.J. Kelly, *Helicobacter pylori* porCDAB and *oorDABC* genes encode distinct pyruvate:-flavodoxin and 2-oxoglutarate: acceptor oxidoreductases which mediate electron transport to NADP, J. Bacteriol. 180 (1998) 1119–1128.
[23] P. Kaihovaara, J. Hook-Nikanne, M. Uusi-Oukari, T.U. Kosunen, M. Salaspuro, Flavodoxin-dependent pyruvate oxidation, acetate production and metronidazole reduction by *Helicobacter pylori*, J. Antimicrob. Chemother. 41 (1998) 171–177.
[24] J. Freigang, K. Diederichs, K.P. Schafer, W. Welte, R. Paul, Crystal structure of oxidized flavodoxin, an essential protein in *Helicobacter pylori*, Protein Sci. 11 (2002) 253–261.

[25] C. Osborne, L.M. Chen, R.G. Matthews, Isolation, cloning, mapping, and nucleotide sequencing of the gene encoding flavodoxin in *Escherichia coli*, J. Bacteriol. 173 (1991) 1729–1737.
[26] S. Wakabayashi, T. Kimura, K. Fukuyama, H. Matsubara, L.J. Rogers, The amino acid sequence of a flavodoxin from the eukaryotic red alga *Chondrus crispus*, Biochem. J. 263 (1989) 981–984.
[27] E.E. Scott, Y.A. He, M.R. Wester, M.A. White, C.C. Chin, J.R. Halpert, E.F. Johnson, C.D. Stout, An open conformation of mammalian cytochrome *P*450 2B4 at 1.6-A resolution, Proc. Natl. Acad. Sci. U. S. A. 100 (2003) 13196–13201.
[28] C.S. Chang, L.T. Chen, J.C. Yang, J.T. Lin, K.C. Chang, J.T. Wang, Isolation of a *Helicobacter pylori* protein, FldA, associated with mucosa-associated lymphoid tissue lymphoma of the stomach, Gastroenterology 117 (1999) 82–88.
[29] C.G. Genzor, A. Beldarrain, C. Gomez-Moreno, J.L. Lopez-Lacomba, M. Cortijo, J. Sancho, Conformational stability of apoflavodoxin, Protein Sci. 5 (1996) 1376–1388.
[30] S. Maldonado, A. Lostao, M.P. Irun, J. Fernandez-Recio, C.G. Genzor, E.B. Gonzalez, J.A. Rubio, A. Luquita, F. Daoudi, J. Sancho, Apoflavodoxin: structure, stability, and FMN binding, Biochimie 80 (1998) 813–820.
[31] A. Lostao, C. Gomez-Moreno, S.G. Mayhew, J. Sancho, Differential stabilization of the three FMN redox forms by tyrosine 94 and tryptophan 57 in flavodoxin from *Anabaena* and its influence on the redox potentials, Biochemistry 36 (1997) 14334–14344.
[32] A. Lostao, M. El Harrous, F. Daoudi, A. Romero, A. Parody-Morreale, J. Sancho, Dissecting the energetics of the apoflavodoxin–FMN complex, J. Biol. Chem. 275 (2000) 9518–9526.
[33] J. Fernandez-Recio, C.G. Genzor, J. Sancho, Apoflavodoxin folding mechanism: an alpha/beta protein with an essentially off-pathway intermediate, Biochemistry 40 (2001) 15234–15245.
[34] C.G. Genzor, A. Perales-Alcon, J. Sancho, A. Romero, Closure of a tyrosine/tryptophan aromatic gate leads to a compact fold in apo flavodoxin, Nat. Struct. Biol. 3 (1996) 329–332.
[35] J.L. Casaus, J.A. Navarro, M. Hervas, A. Lostao, M.A. De la Rosa, C. Gomez-Moreno, J. Sancho, M. Medina, *Anabaena* sp. PCC 7119 flavodoxin as electron carrier from photosystem I to ferredoxin-$NADP^+$ reductase. Role of Trp(57) and Tyr(94), J. Biol. Chem. 277 (2002) 22338–22344.
[36] M.L. Ludwig, K.A. Pattridge, A.L. Metzger, M.M. Dixon, M. Eren, Y. Feng, R.P. Swenson, Control of oxidation–reduction potentials in flavodoxin from *Clostridium beijerinckii*: the role of conformation changes, Biochemistry 36 (1997) 1259–1280.
[37] S.G. Mayhew, M.L. Ludwig, Flavodoxins and Electron Transferring Flavoproteins, Academic Press, New York, 1975.
[38] F.C. Chang, R.P. Swenson, Regulation of oxidation–reduction potentials through redox-linked ionization in the Y98H mutant of the *Desulfovibrio vulgaris* [*Hildenborough*] flavodoxin: direct proton nuclear magnetic resonance spectroscopic evidence for the redox-dependent shift in the pKa of Histidine-98, Biochemistry 36 (1997) 9013–9021.
[39] D.H. Kwon, M.S. Osato, D.Y. Graham, F.A. El-Zaatari, Quantitative RT-PCR analysis of multiple genes encoding putative metronidazole nitroreductases from *Helicobacter pylori*, Int. J. Antimicrob. Agents 15 (2000) 31–36.
[40] S.G. Mayhew, V. Massey, Purification and characterization of flavodoxin from *Peptostreptococcus elsdenii*, J. Biol. Chem. 244 (1969) 794–802.
[41] J.F. Brandts, L.N. Lin, Study of strong to ultratight protein interactions using differential scanning calorimetry, Biochemistry 29 (1990) 6927–6940.
[42] M.W. Pantoliano, E.C. Petrella, J.D. Kwasnoski, V.S. Lobanov, J. Myslik, E. Graf, T. Carver, E. Asel, B.A. Springer, P. Lane, F.R. Salemme, High-density miniaturized thermal shift assays as a general strategy for drug discovery, J. Biomol. Screen. 6 (2001) 429–440.
[43] T.T. Waldron, K.P. Murphy, Stabilization of proteins by ligand binding: application to drug screening and determination of unfolding energetics, Biochemistry 42 (2003) 5058–5064.
[44] J. Fernandez-Recio, A. Romero, J. Sancho, Energetics of a hydrogen bond (charged and neutral) and of a cation/pi interaction in apoflavodoxin, J. Mol. Biol. 290 (1999) 319–331.
[45] I. Luque, E. Freire, Structural parameterization of the binding enthalpy of small ligands, Proteins 49 (2002) 181–190.
[46] M.J. Todd, E. Freire, The effect of inhibitor binding on the structural stability and cooperativity of the HIV-1 protease, Proteins 36 (1999) 147–156.
[47] T. Wiseman, S. Williston, J.F. Brandts, L.N. Lin, Rapid measurement of binding constants and heats of binding using a new titration calorimeter, Anal. Biochem. 179 (1989) 131–137.
[48] A.E. Eriksson, W.A. Baase, J.A. Wozniak, B.M. Matthews BW, A cavity-containing mutant of T4 lysozyme is stabilized by buried benzene, Nature 355 (1992) 371–373.
[49] M. Kidd, A.J. Lastovica, J.C. Atherton, J.A. Louw, Heterogeneity in the *Helicobacter pylori vacA* and *cagA* genes, Gut 45 (1999) 499–502.
[50] S.J. Spechler, L. Fischbach, M. Feldman, Clinical aspects of the genetic variability in *Helicobacter pylori*, JAMA 283 (2000) 1264–1266.
[51] H. Rautelin, K. Seppala, O.V. Renkonen, U. Vainio, T.U. Kosunen, Role of metronidazole resistance in therapy of *Helicobacter pylori* infections, Antimicrob. Agents Chemother. 36 (1992) 163–166.
[52] D.I. Edwards, Nitroimidazole drugs-action and resistance mechanisms: I. Mechanisms of action, J. Antimicrob. Chemother. 31 (1993) 9–20.
[53] D.I. Edwards, Nitroimidazole drugs-action and resistance mechanisms: II. Mechanisms of resistance, J. Antimicrob. Chemother. 31 (1993) 201–210.